Biosensors and Bioelectronics 25 (2010) 2026–2032

Contents lists available at ScienceDirect

Biosensors and Bioelectronics

journal homepage: www.elsevier.com/locate/bios

An efficient non-mediated amperometric biosensor for nitrite determination

Célia M. Silveira[a], Sofia P. Gomes[b], Alberto N. Araújo[b], M. Conceição B.S.M. Montenegro[b], Smilja Todorovic[c], Ana S. Viana[d], Rui J.C. Silva[e], José J.G. Moura[a], M. Gabriela Almeida[a,f,*]

[a] REQUIMTE – Dept. de Química, CQFB, Faculdade de Ciências e Tecnologia, Universidade Nova de Lisboa, 2829-516 Caparica, Portugal
[b] REQUIMTE – Dept. de Química-Física, Faculdade de Farmácia, Universidade do Porto, R. Aníbal Cunha, 164, 4099-030 Porto, Portugal
[c] ITQB, Universidade Nova de Lisboa, 2780-157 Oeiras, Portugal
[d] Centro de Química e Bioquímica, Faculdade de Ciências da Universidade de Lisboa, Campo Grande, 1749-016 Lisboa, Portugal
[e] CENIMAT/I3N – Faculdade de Ciências e Tecnologia, Universidade Nova de Lisboa, 2829-516 Caparica, Portugal
[f] Escola Superior de Saúde Egas Moniz, Monte de Caparica, 2829-511 Caparica, Portugal

ARTICLE INFO

Article history:
Received 7 January 2010
Accepted 25 January 2010
Available online 6 February 2010

Keywords:
Cytochrome *c* nitrite reductase
Sol–gel
Direct electrochemistry
Nitrite
Biosensor

ABSTRACT

In this paper we propose the construction of a new non-mediated electrochemical biosensor for nitrite determination in complex samples. The device is based on the stable and selective cytochrome *c* nitrite reductase (ccNiR) from *Desulfovibrio desulfuricans*, which has both high turnover and heterogeneous electron transfer rates. In opposition to previous efforts making use of several redox mediators, in this work we exploited the capacity of ccNiR to display a direct electrochemical response when interacting with pyrolytic graphite (PG) surfaces. To enable the analytical application of such bioelectrode the protein was successfully incorporated within a porous silica glass made by the sol–gel process. In the presence of nitrite, the ccNiR/sol–gel/PG electrode promptly displays catalytic currents indicating that the entrapped ccNiR molecules are reduced via direct electron transfer. This result is noteworthy since the protein molecules are caged inside a non-conductive silica network, in the absence of any mediator species or electron relay. At optimal conditions, the minimum detectable concentration is 120 nM. The biosensor sensitivity is 430 mA M^{-1} cm^{-2} within a linear range of 0.25–50 μM, keeping a stable response up to two weeks. The analysis of nitrites in freshwaters using the method of standard addition was highly accurated.

1. Introduction

The last decades have witnessed a budding demand for improved analytical tools to enable the reliable inspection of the chemical or biological composition of every material that interacts with Consumers or Nature. In this context, biosensor technology constitutes a very important field of Research and Development. Electrochemical enzyme based biosensors are of particular interest due to their operational simplicity, low cost fabrication, portability and real-time monitoring ability. However, it is often hard to achieve an efficient electronic communication between the enzyme and the signal transducer since the limited exposure of the redox active sites prevents facile electron transfer (ET) towards the electrode. Several approaches have been proposed to solve this issue. In the first generation of biosensors, the strategy relies on the measurement of an electroactive substrate or product of the enzymatic reaction while in second generation devices the reaction is monitored by a natural or artificial redox mediator. Major improvements, such as the elimination of mediator leakage, were obtained with the introduction of a third generation of biosensors where the redox communication is ensured by enzyme wiring or electron relays (Wang, 1999a; Willner et al., 2006). Yet, the ideal approach allows direct electron transfer (DET) between the oxidoreductase and the electrode, thereby increasing selectivity, simplifying the manufacturing process and requiring fewer reagents (Gorton et al., 1999; Wu and Hu, 2007). However, the protocols for enzyme immobilization are still a challenge in the field of DET based biosensors. Among the limited number of examples found in the literature, heme containing proteins (e.g. myoglobin, hemoglobin and peroxidases) prevail, probably due to their greater stability and high heterogeneous electron transfer rates (Gorton et al., 1999).

In this work we propose the construction of a truly non-mediated amperometric biosensor for nitrites (NO_2^-) determination. This analyte is commonly present in many different moieties. On top of its natural occurrence in environmental and physiological systems, nitrite has been used for centuries as fertilizer and food preservative (E249-250). Recently, the issue of its potential toxicity has come forward and generated the implemen-

* Corresponding author at: REQUIMTE – Dept. de Química, CQFB, Faculdade de Ciências e Tecnologia, Universidade Nova de Lisboa, 2829-516 Caparica, Portugal. Tel.: +351 212948550; fax: +351 212948300.
E-mail address: mga@dq.fct.unl.pt (M.G. Almeida).

0956-5663/$ – see front matter © 2010 Elsevier B.V. All rights reserved.
doi:10.1016/j.bios.2010.01.031

tation of rules to restrict its level in drinking waters [98/83/EC] and food products [2006/52/EC]. Although several analytical techniques have been proposed for nitrite quantification (review by Moorcroft et al., 2001), they have shown important limitations such as sample pre-treatment stages, susceptibility to matrix interferences, insufficient detection limits and lack of portability. Consequently, the development of a sensor device using a highly selective, active and stable biocatalyst seems to be a reliable option for nitrite detection in complex media. In fact, some attempts to construct a nitrite biosensor were recently proposed by our group and collaborators. For this, we have been using the multihemic cytochrome *c* nitrite reductase (*cc*NiR) from *Desulfovibrio desulfuricans* ATCC 27774 as the biorecognition element, which performs the fast six electron reduction of nitrite to ammonia. The catalytic reaction occurs at a high-spin (5-coordinated) heme that is located at a pentahemic subunit of 61 kDa (α) which is strongly bound to its physiological electron donor, a smaller hydrophobic polypeptide tetrahemic of 19 kDa (β), composed of 4 *c*-types hemes; *in vitro*, the protein complexes associate each other forming huge aggregates (*min*. 890 kDa) (Almeida et al., 2003). As transducing elements, different amperometric electrodes were designed using a variety of immobilization materials, such as electropolymerized films (Silva et al., 2004), non-conducting polymers (Almeida et al., 2007a), and redox active layered double hydroxides (Chen et al., 2007). Quite recently, a conductimetric transduction approach was also proposed (Zhang et al., 2009). All of these systems share the use of artificial electroactive compounds as electron shuttles. Recent results have shown that *cc*NiR is also able to display a DET response when simply adsorbed onto a pyrolytic graphite electrode (PGE) (Almeida et al., 2007b). To construct a suitable analytical device based on this system, enzyme incorporation in a protective matrix is strongly recommended. This may provide the protein with greater stability and act as a barrier against fouling and interfering species. However, the high molecular weight of the *cc*NiR aggregates and their partial hydrophobic character may hamper the encapsulation process.

In this paper we describe a successful way of entrapping *cc*NiR in a porous membrane losing neither the catalytic activity nor the direct electronic contact with the electrode surface. The method is based on the encapsulation of the protein within a sol–gel matrix, a versatile material usually compatible with biological activity and with the easy diffusion of small substrate molecules. The sol–gel formation is a mild procedure and the properties of the final framework (diffusion within the matrix, porous structure, thickness, etc.) may be modulated by the chemical nature of the precursors, the water : silane molar ratio, the reaction medium and the enzyme concentration (Dave et al., 1994; Lev et al., 1995; Wang, 1999b). All these parameters were optimized earlier in this work. As sol–gel precursors the quite hydrophobic tetraethoxysilane (TEOS) and 2-(3,4-epoxycyclohexyl)-ethyltrimethoxy silane (EETMS) were tested (Pandey et al., 1999a,b). Taking into account the large dimensions of the *cc*NiR aggregates, all the recipes started from high water : silane molar ratios.

2. Materials and methods

2.1. Reagents

All chemicals were analytical grade and used without further purification. Solutions were prepared with deionized water (18 MΩ cm) from a Millipore MilliQ water purification system. The sol–gel precursors EETMS and TEOS were obtained from Fluka. Hydroxylamine and methyl viologen were purchased from Sigma. Sodium nitrite, sodium sulphite, ammonium chloride, tris(hydroxymethyl)aminomethane, potassium chloride, sodium hydrogenphosphate and sodium dihydrogenphosphate were from Merck. Ethanol was from Panreac and hydrochloric acid from Riedel-de-Haen.

*cc*NiR was purified from *D. desulfuricans* ATCC 27774 as previously described (Almeida et al., 2003). The specific activity was 300 U/mg (1 U–1 μmol nitrite reduced *per* minute), the turnover number was 340 s^{-1} (20 °C) and the protein content was 1.0 mg/mL, in 0.05 M phosphate buffer, pH 7.6.

2.2. Enzyme assays

The enzymatic activity was determined following the oxidation of methyl viologen, previously reduced with zinc, at 604 nm (ε = 13.6 mM^{-1} cm^{-1}), using a Diode array spectrophotometer (Agilent Techonologies 8453A UV–Vis). The assay mixture contained 0.16 mM methyl viologen and 0.6 nM *cc*NiR in 0.3 M phosphate buffer, pH 7.6. The reaction was started by the addition of nitrite. All assays were performed anaerobically, at 20 °C.

2.3. Electrochemical measurements

A conventional three-electrode electrochemical cell was used, with an Ag/AgCl reference electrode, a Pt counter electrode and a self-made PGE (Φ = 4 mm) modified with the enzyme/sol–gel film, as working electrode. The electrochemical cell, containing 20 mL of 0.1 M KCl in 0.05 M Tris–HCl buffer, pH 7.6 as supporting electrolyte, was thoroughly purged with argon before and during the experiments. Measurements were performed with a potentiostat Autolab PSTAT 12 (Eco-Chemie) monitored by the control and data acquisition software GPES 4.9. In cyclic voltammetry experiments, a 20 mV/s scan rate was used. To evaluate the biosensors response to nitrite, the electrochemical cell was successively spiked with a standard solution. For amperometric experiments the electrode was settled at −0.9 V, with a speed rotation of 600 rpm (kinetic studies) or argon bubbling (calibration). Unless stated otherwise, all potentials were quoted against the Ag/AgCl reference electrode.

2.4. Bioelectrode preparation

Prior to coating, the PGEs were polished with alumina slurry (0.3 μm). The electrodes were then thoroughly washed with water and ethanol and ultrasonicated for 5 min. Finally, the electrodes were washed with water and dried with compressed air.

The TEOS sol–gel mixtures were prepared by mixing different molar ratios of water and precursor (50:1; 250:1 and 500:1) with 8% ethanol and 10 mM HCl. The same was done for the EETMS containing mixtures, using 40:1, 225:1 and 450:1 H_2O : silane ratios, 11% ethanol and 2 mM HCl (a detailed description of these formulations is presented in Supplementary Data file, in conjunction with some other sol–gel recipes tested without success). The mixtures were magnetically stirred for 30 min. (for the TEOS based preparations, an ice bath was used to prevent premature gel formation). Next, a drop of 10 μL was placed onto the PGE and left at room temperature, for sol development (*ca.* 45 min.). Before starting the gelation process, the sol layer was impregnated with enzyme solution (15–92 pmol) and left for a 24 h aging period, at room temperature. The modified electrodes were finally washed and stored in supporting electrolyte at 4 °C.

2.5. Characterization of the ccNiR/sol–gel film

The scanning electron microscopy (SEM) analysis were performed in a Zeiss model DSM 962, with a secondary electrons detector (SE) and an energy dispersive X-ray spectrometer (EDS) from Oxford Instruments model INCAx-sight with an ultra thin

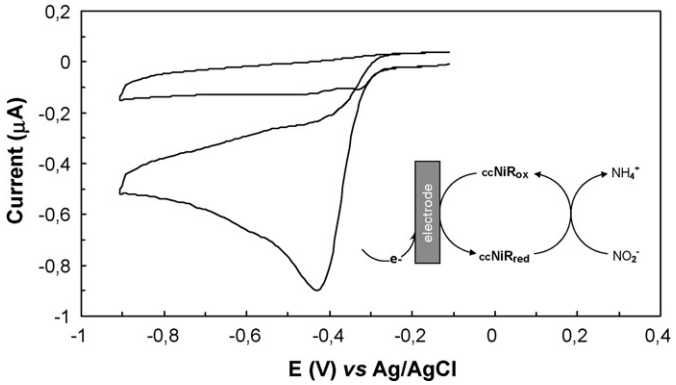

Fig. 1. Cyclic voltammograms with (10 μM) and without nitrite. The sol–gel was prepared with the optimal composition 225:1 H_2O : EETMS molar ratio and 74 pmol of *cc*NiR. Inset: schematic representation of the reaction mechanism that describes the voltammograms profile, i.e., the enzyme undergoes a reversible electrochemical reduction followed by an irreversible chemical reaction (EC').

window able to detect low atomic number elements. The electrode surface was previously coated with gold to increase electrical conductivity during examination.

Tapping mode AFM images were obtained in a Multimode Nanoscope IIIa Microscope (Digital Instruments, Veeco) in air, using etched silicon cantilevers with spring constants of *ca.* 300 kHz (Tap300, BudgetSensors). The images were acquired at a scan rate of 1.5–1.8 Hz.

The electronic absorption spectra were obtained at a Shimadzu UV-1800 spectrophotometer. The protein doped glass slides were prepared on top of the inner face of a quartz cuvette (UV–Vis). After sol–gel aging, the cuvette was filled up with electrolyte solution. Resonance Raman (RR) measurements were performed with a confocal microscope coupled to a Raman spectrometer (Jobin Yvon U1000) equipped with 1200 l/mm grating and liquid-nitrogen-cooled back-illuminated CCD detector. The *cc*NiR containing glass slides were formed on microscopic lamellas. Following the sol–gel aging period, the samples were excited with the 413 nm line from a krypton ion laser (Coherent Innova 302). RR spectra of hydrated sample were measured with variable (750 μW–1.5 mW) laser power and (10–40 s) accumulation time, at RT, at different spots on the matrix. Experimental RR spectra, that represent an average of 4–10 spectra taken from different spots, were submitted to component analysis by a home made software.

3. Results and discussion

3.1. Biosensor optimization

The optimum membrane composition was selected from a group of sol–gel/*cc*NiR formulations prepared with different precursors, water : monomer molar ratios and enzyme quantities. The bioelectrodes were characterized by cyclic voltammetry since a typical catalytic shape current–potential curve was always observed in the presence of nitrite (Fig. 1) due to the non-mediated electroenzymatic reduction of the substrate, according with the EC' mechanism depicted in the inset of Fig. 1.

In control experiments using sol–gel modified electrodes without *cc*NiR (not shown), no catalytic reaction was detected upon analyte addition. The analytical performance was evaluated according to the sensitivity to nitrite, the detection limit and the amplitude of the linear range. Table 1 summarizes the results concerning the effects of the nature and amount of the sol–gel precursor.

Regarding the TEOS based formulations, the linear range did not change much with the decreasing amount of silane whereas the sensitivity fell progressively, especially from 250:1 to 500:1 H_2O : TEOS, most likely because the silica pores were too big to withhold the protein molecules. All biosensing films had a thin and glassy appearance but a high tendency to fracture during the drying process, occasionally loosing small pieces of glass. As a consequence, the reproducibility was rather low and TEOS was discarded.

When using EETMS, the modified electrodes were smooth and shiny after the sol–gel development period (24 h), although the surface became a bit cracked once the aging process took place, as later confirmed by SEM [this has been shown to be related with the EETMS hydrophobicity that generates small wettable areas and brittle surfaces (Lev et al., 1995; Pandey et al., 1999a,b)]. These results not only were slightly better than those obtained with TEOS, they were much more reproducible. This formulation also displayed the highest catalytic efficiency, expressed as the quotient between the peak reduction currents in the presence and absence of nitrite (Table 1). Due to the presence of the bulky epoxy-cyclohexyl group, EETMS is likely to decrease the rate of hydrolysis and condensation (Lev et al., 1995), producing a more adequate network for both enzyme encapsulation and DET. The composition with the lowest water content (40:1 H_2O : EETMS) gave the poorest analytical parameters, marked by an abnormally low sensitivity to nitrite (Table 1). Several factors could account for this situation: (i) the low amount of water produced pores too small to accommodate the large size aggregates of *cc*NiR and/or generated an extremely strong barrier to nitrite diffusion, as judged by the extensive linear range; (ii) the sol–gel polymerization under a low water : silane ratio stimulated enzyme aggregation, producing lower activities; (iii) the reduced wettability of the film decreased both capacitive and Faradaic currents (Pandey et al., 1999c). In opposition, as suggested by the lower sensitivities and narrower linear ranges seen in Table 1, the highest H_2O : silane ratio (450:1) produced pores too large in size and the enzyme encapsulation was less efficient. A good balance between sensitivity to nitrite and linear range amplitude was obtained with the formulation based on the 225:1 ratio.

Thereafter, several electrode configurations using the latter H_2O : EETMS combination and varying amounts of *cc*NiR (from 30 to 735 pmol cm^{-2}) were tested. The linear range is wider when using a surface concentration of 590 pmol cm^{-2} while the biosensor sensitivity to nitrite reaches a maximum at 120 pmol cm^{-2}, stays fairly constant up to 590 pmol cm^{-2} and then has a significant drop off (Fig. S1, Supplementary Data). This reduction of activity at high enzyme loadings could be related to a hyperaggregation of the protein complexes within the sol–gel network and/or to a much slower diffusion of the substrate across the highly doped ceramic mate-

Table 1
Analytical properties of *cc*NiR/sol–gel based nitrite biosensors prepared with TEOS and EETMS, in different water : silane proportions.

Precursor	Water : precursor molar ratio	Linear range (NO_2^- μM)	Sensitivity (mA M^{-1} cm^{-2})	I_{cat}/I_c
TEOS	50:1	0.5–20/40	311 ± 41	3.5 ± 0.4
	250:1	0.5–25/40	261 ± 20	1.4 ± 0.1
	500:1	0.5–25/35	69 ± 25	1.6 ± 0.2
EETMS	40:1	20/200–2000	0.054 - 0.24	N.D.
	225:1	0.25–50	430 ± 23	6.6 ± 1.1
	450:1	0.25–5	274 ± 34	1.9 ± 0.2

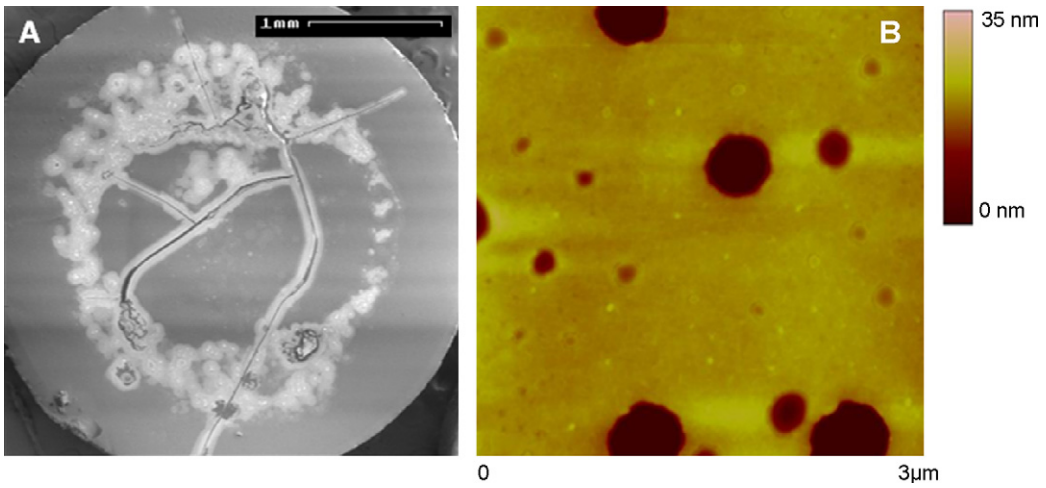

Fig. 2. Morphological characterization of the surface of a *cc*NiR doped sol–gel film, prepared with 74 pmol of enzyme and a 225:1 H_2O : EETMS molar ratio. (A) SEM micrograph (signal amplification ×22, 5 kV). (B) AFM image of a selected area.

rial (Pandey et al., 1999b). For further studies, we selected a *cc*NiR amount of 590 pmol cm^{-2} (74 pmol) since it combined a good sensitivity with a broader linearity window and better reproducibility.

The *cc*NiR/sol–gel films obtained in the optimized conditions were structurally characterized and the analytical performance of the bioelectrodes was further evaluated by amperometry.

3.2. Characterization of the *cc*NiR/sol–gel membrane

3.2.1. Morphology

The global inspection of the modified *cc*NiR/sol–gel electrode by SEM (Fig. 2A) reveals a very smooth surface, randomly interrupted by cracks.

The film is partially covered by layers of deposited materials that also surround the sol–gel fissures. According to the SEM-EDS analysis (Fig. S2, Supplementary Data), these deposits are particularly rich in P, K and O elements, probably coming from the phosphate salts (K_2HPO_4 and KH_2PO_4) that compose the buffer solution. Results suggest that this salt solution is expelled from the silica network essentially through the sol–gel cracks, forming small pools that, upon drying, create salt deposits. This phenomenon was not seen on control films where the enzyme solution was replaced by an equal volume of deionized water (not shown). Therefore, it can be concluded that the presence of phosphate salts stimulates cracking in EETMS based silicas. This is understandable since this ceramic material has a strong hydrophobic character. Nevertheless, one should be aware that this effect may seem particularly accentuated due to the longer sol–gel drying period (*ca.* 72 h) imposed by the SEM analysis. For biosensing purposes, the bioceramic film was not allowed to dry for such a long time. So, the formation of cracks and salt deposits should be less important in this case. Surprisingly, in spite of the fact that phosphate salts are a frequent component of enzyme containing solutions used in the construction of sol–gel based biosensors, to our knowledge, the rejection of these salts from silicate films was never reported before. A closer look to the micrograph demonstrates that although the electrode coverage is not completely uniform, ordered microstructure areas may be found. Some of these zones were further investigated using AFM (a selected example is shown in Fig. 2B). In all the inspected regions the surface was rather flat and there was no evidence of large protein aggregates outside the silica layer, suggestive of an effective enzyme entrapment inside the silica network. The *cc*NiR/silicate surface showed both large and small pores, ranging from an upper diameter of about 1 μm down to tens of nanometers. This heterogeneity was not caused by protein incorporation since sol–gel films prepared in its absence were also characterized by a nano- to submicroporosity (not shown).

3.2.2. Spectroscopy

In order to inspect the effect of the immobilization procedure on the structural integrity the hemes co-factors of *cc*NiR, enzyme doped sol–gel films were examined by spectroscopic techniques.

The UV–Vis spectra of the entrapped *cc*NiR, in both oxidized and dithionite reduced forms (Fig. 3A), are quite similar to the ones observed in solution (Almeida et al., 2003).

In fact, the spectroscopic features assigned to *c*-type hemes (Soret, Q, α and β bands) did not change upon protein encapsulation, keeping constant both wavelength maxima and band width. The only difference resides in a decrease of peak intensity of the Soret band (410 nm). In light of the fact that protein unfolding induces visible alterations in the hemes spectroscopic signature in terms of position, intensity and broadening (Dave et al., 1997), the obtained data give good indications about the biocompatibility of the microenvironment produced by the EETMS based silica matrix. Resonance Raman data also support these findings (Fig. 3B). Namely, the high frequency region spectra of the encapsulated *cc*NiR obtained under Soret excitation revealed typical features of a multiple *c*-type heme containing protein. The frequencies of the heme oxidation and spin state marker bands, ν_3 (1504 cm^{-1}), ν_2 (1587 cm^{-1}) and ν_{10} (1637 cm^{-1}) indicate that the predominant species is in the low spin (LS) state, as expected. Component analysis revealed the presence of high spin (HS) species with down-shifted frequencies at 1367 cm^{-1} and 1495 cm^{-1} for ν_4 and ν_3 modes, respectively. The observed frequencies for both HS and LS modes are in agreement with those found in solution RR spectra of *cc*NiR (not shown), and the values reported for *bis*-His and 5-coordinated HS hemes *c* (Siebert and Hildebrandt, 2008). Therefore, no indications of denaturation or conformational changes of heme groups upon encapsulation of *cc*NiR into the sol–gel matrix were detected in the RR spectra. A shoulder at 1360 cm^{-1} in the experimental spectrum originates from partial photoreduction of the protein; the intensity of this band is in direct correlation with the exposure of the sample to the laser beam, being present in the spectra even for the shortest accumulation times and laser power.

3.2.3. Electrochemistry

In the absence of nitrite, a very small non catalytic peak was observed (Fig. 1). This attests for the extraordinary capacity of *cc*NiR to exchange electrons directly with the solid electrode, especially if one considers that the large enzyme aggregates are randomly

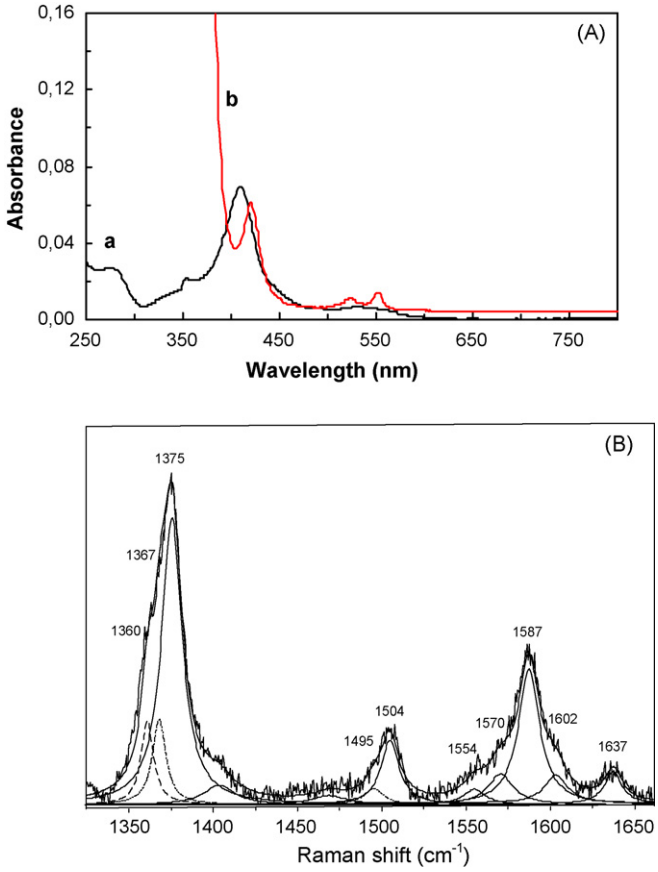

Fig. 3. Spectroscopic characterization of the ccNiR doped glass slide. (A) UV/Vis spectra of a slide hydrated in supporting electrolyte, in the oxidized (a) and dithionite reduced (b) forms. (B) Experimental and component resonance Raman spectra. Experimental spectrum is an average of 4, measured from different spots on the surface with 413 nm excitation, 20 s accumulation time and 750 mW laser power. The most prominent oxidation/spin state marker bands are indicated; dotted bands (1367 cm^{-1} and 1495 cm^{-1}) are assigned to the high spin species and dashed band to photoreduced protein.

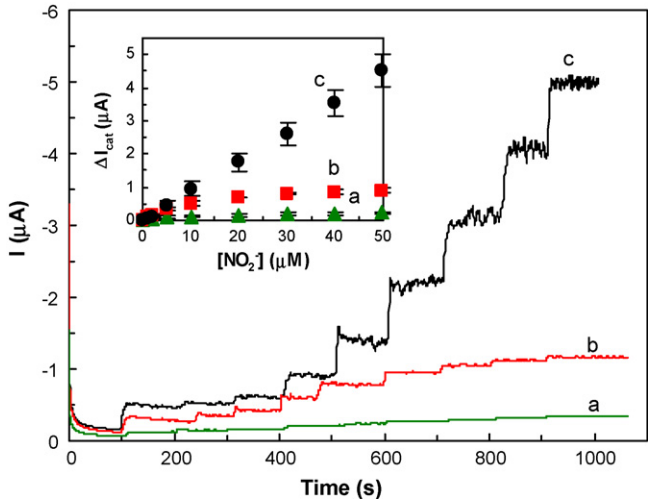

Fig. 4. Biosensor response to nitrite addition using the ccNiR/sol–gel formulation, 74 pmol of enzyme and 225:1 H_2O : EETMS molar ratio. Amperometric measurements and corresponding calibration curves (inset) registered at different working potentials: (a) −0.5 V; (b) −0.7 V; (c) −0.9 V *vs* Ag/AgCl. The maximum limit of the linear range is 2 μM for −0.5 V, 10 μM for −0.7 V, and 50 μM for −0.9 V.

oriented inside a non-conductive silica matrix. The signal appears in the same potential region of the broad wave previously identified when using ccNiR directly adsorbed on a PG electrode (Almeida et al., 2007b). The absence of a peak shift upon entrapment suggests that this process did not significantly disturb the formal potential of the protein co-factors. However, the corresponding anodic peak was difficult to detect and the peak definition at all the tested scan rates was rather poor. These setbacks hindered a detailed analysis of the electrochemical process and eventual assessment of valuable parameters such as protein coverage and heterogeneous electron transfer rate constants.

3.3. Response to nitrite

To settle the operating potential for the bioelectrode calibration, amperometric measurements were carried out at three different voltages, all of them close to or well below the reduction potential of the catalytic heme (≈−0.42 V, pH 7) i.e., the site of interaction with the substrate (Almeida et al., 2007b). In this way, the supply of the minimal reduction power needed for enzyme activity is guaranteed. Nevertheless, some of the remaining hemes from both subunits have reduction potentials above −0.42 V. This may provide extra electron tunnelling pathways between the active site and the enzyme surface, contributing to the amplification of heterogeneous ET. Fig. 4 shows the amperometric responses and corresponding calibration curves obtained at −0.5, −0.7 and −0.9 V. The amperometric response upon nitrite addition was always prompt and reached a maximum within 5 s, indicative of a sufficiently fast heterogeneous ET.

Although the enzyme co-factors are only slightly reduced, a small electrocatalytic activity could be detected at the highest voltage tested (−0.5 V). As the reduction potential decreased the linear response of the biosensor towards nitrite became wider. In fact, the electrode subjection to a stronger driving force helped interfacial ET and increased enzyme reduction, promoting catalytic activity. However, the probability of having background interference from complex samples increases at very negative potentials and sample degassing is mandatory to eliminate the interference from oxygen. In this regard, a less negative working potential is preferred. Since the sensitivity of the biosensor through a range of different voltages is quite similar (*ca.* 10% variation), one can adjust the working potential as a balance between the desired quantification limits and the interferences risks. For further analytical characterizations, we decided in favour of the broader analytical performance of the bioelectrode, i.e., a potential of −0.9 V. At this voltage, the response of the biosensor to the enzyme substrate was linear from 0.25 to 50 μM, the detection limit was 120 nM (at a signal-to-noise ratio of 3) and the sensitivity (given by the slope of the calibration curve), was $430 \pm 23\ mA\ M^{-1}\ cm^{-2}$. The sensitivity variation between electrode preparations was less than 11%. This fluctuation is most likely related to the enzyme immobilization method, given that it consists on the simple cast of ccNiR/sol–gel drops on top of the electrode. The reproducibility of the electrocatalytic response depends on the exact amount of protein entrapped within the sol–gel layer and, very importantly, on the proper orientation of the protein molecules towards the electrode surface, which can vary from preparation to preparation (Dave et al., 1997; Gorton et al., 1999).

To determine the kinetic parameter K_m of ccNiR in the immobilized state, the amperometric analysis was repeated using a rotating electrode, in order to avoid mass transport control (Fig. S3 Suppl. Data). For nitrite concentrations above 100 μM, the plot of catalytic current *vs* nitrite concentration reaches a pseudo-plateau consistent with a Michaelis–Menten enzyme kinetics. According to the data fitting, the K_m^{app} is 27 ± 1 μM, 7.5 times higher than the value determined in bulk solution (3.6 μM, 20 °C) and almost 4 times the one previously obtained from non-

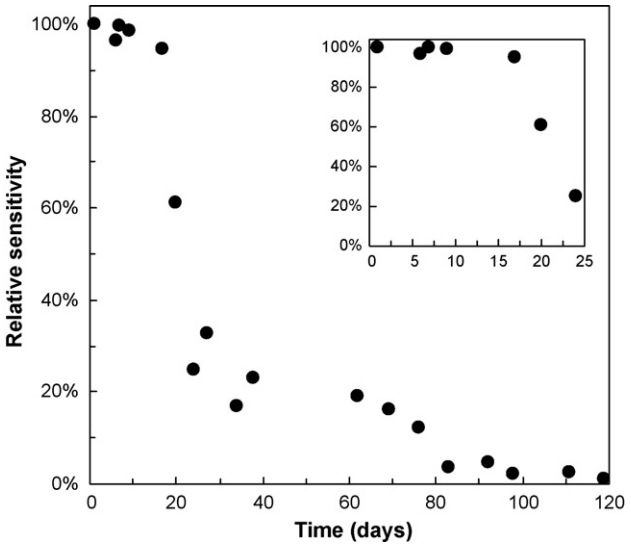

Fig. 5. Effect of time on the biosensor sensitivity for nitrite determination. Sensitivity values were given by the slope of calibration curves performed periodically throughout 120 days. The electrode had a *cc*NiR/sol–gel formulation of 74 pmol of enzyme and 225:1 H_2O: EETMS molar ratio. Catalytic currents were measured at −0.9 V *vs* Ag/AgCl.

encapsulative direct electrochemistry (7 μM, 20 °C) (Almeida et al., 2007b). The increasing factor of the Michaelis constant is typical for immobilized enzymes and it is attributed to the creation of a barrier to substrate diffusion by the host matrix, in this case, the sol–gel layer. Thus, we consider it to be very unlikely that the affinity for the substrate has been significantly affected by the immobilization procedure.

3.4. Interferences

The biosensor response to potential interferences was studied by comparing the magnitude of the catalytic response to 20 μM nitrite with the one obtained after adding the same concentration of a second chemical species. In this way, the bioelectrode did not show any activity for nitrate ions (NO_3^-) which are often present in nitrite containing samples. Also, no catalytic response was observed for sulphite (SO_3^{2-}), although for higher concentrations a small inhibition effect was detected (−2.5%). Ammonium (NH_4^+), the final product of nitrite reduction by *cc*NiR, did not affect the biosensor response either. In the presence of hydroxylamine (NH_2OH), the bioelectrode increased its response by 1.2%. This is a very low value when compared with other *cc*NiR based biosensing systems (Almeida et al., 2007a). Hence, the *cc*NiR/sol–gel biosensor has drastically diminished the hydroxylamine interference. The explanation for such a low activity is unclear for now, but it is probably related to the specificities of the silica matrix and its interactions with the substrate molecules.

3.5. Stability

The *cc*NiR/sol–gel modified electrodes were stored in Tris–HCl buffer, pH 7.6, at 4 °C, and tested for stability. Calibration curves were periodically traced and the linear range and sensitivity for nitrite were evaluated as shown in Fig. 5.

In spite of a nearly daily utilization, both the linear range and sensitivity of the biosensor were quite stable (>90%) during the first two weeks. Thus, the silica matrix hosts the enzyme in a biocompatible cage, simultaneously preventing denaturation and lixiviation. Thereafter, the biosensor activity started to decrease progressively, keeping just 15% of the initial activity after thirty days. This deteriorating response is most likely due to the enzyme inactivation, related (or not) to the sol–gel aging process. Interestingly, the bioelectrode retained a residual electrocatalytic activity over an extremely long period of time (up to six months, not shown).

3.6. Application

The *cc*NiR/sol–gel biosensor was used to determine the concentration of nitrite in two real samples (A and B) collected from surface waters of a Portuguese river, without any treatment, using the method of standard addition and the procedure described in Section 2.3. Each sample was examined in three independent assays ($n = 3$), using two different bioelectrode assemblies. The obtained results (A, 2.12 ± 0.14 and B, 11.47 ± 0.26 μM) were quite similar to the values obtained by the colorimetric method (A, 2.13 and B, 11.44 μM) described in the Standard Methods for the Examination of Water and Wastewater (4500-NO_2^-, B). This experiment attests the high accuracy of the analysis and indicates that the proposed biosensor can be reliably applied to the nitrite determination in freshwaters.

4. Conclusions

Due to the inherent properties of *cc*NiR and to the tunable porosity and hydrophobicity of the silica immobilizing layers it was possible to achieve a direct electrochemical response of *cc*NiR when coupled to pyrolytic graphite interfaces. In this way, one could construct an absolutely non-mediated biosensing system that provides an efficient and very elegant way for assessing nitrites. The *cc*NiR/sol–gel biosensor displays a good analytical performance when compared to the formerly proposed bioelectrodes (Almeida et al., 2007a; Chen et al., 2007; Silva et al., 2004; Zhang et al., 2009). The enhanced selectivity towards nitrite and the high stability of operation clearly constitute the most important advances. The sensitivity is satisfactory and the LOD is well below the EU rules for nitrite in drinking waters (2.2 μM).

Furthermore, the proposed biosensing system is easier to fabricate and works as a starting platform that can be modulated as a function of the analytical requirements. In particular, those parameters influenced by the analyte mass transport can be tuned by simply adjusting the diffusional barrier (e.g., depositing an additional polymeric layer).

A drawback faced by encapsulation approaches when associated to DET is the lack of control of the spatial arrangement of the protein molecules, lowering both electronic communication and reproducibility. The development of a reliable nitrite amperometric biosensor for mass production should overcome this issue. In this regard, the proposed device shows great potential for improvement due to the versatility of the sol–gel chemistry for imparting geometric order to entrapped molecules. A promising strategy is silica functionalization via introduction of mercapto-groups used for protein anchoring.

The elimination of oxygen interferences is another pending question. Again, further developments of the *cc*NiR/sol–gel system may optimize the working potential of the proposed biosensor since it offers some chances to operate at reduction potentials slightly above oxygen reduction. Perhaps an improved interfacial ET may decrease the driving force needed for enzyme activation.

Acknowledgments

The authors thank the financial support from REQUIMTE and Fundação para a Ciência e Tecnologia (Ph.D. fellowships SFRH/BD/13653/2003, SFRH/BD/28921/2006 and Project

POCI/QUI/58026/2004) and to Eng. Susel Caetano, from Laboratório de Análises do Instituto Superior Técnico, for giving us the river samples and quantifying their nitrite content.

Appendix A. Supplementary data

Supplementary data associated with this article can be found, in the online version, at doi:10.1016/j.bios.2010.01.031.

References

Almeida, M.G., Macieira, S., Gonçalves, L.L., Huber, R., Cunha, C.A., Romão, M.J., Costa, C., Lampreia, J., Moura, J.J., Moura, I., 2003. Eur. J. Biochem. 270 (19), 3904–3915.
Almeida, M.G., Silveira, C.M., Moura, J.J., 2007a. Biosens. Bioelectron. 22, 2485–2492.
Almeida, M.G., Silveira, C.M., Guigliarelli, B., Bertrand, P., Moura, J.J., Moura, I., Leger, C., 2007b. FEBS Lett. 581, 284–288.
Chen, H., Mousty, C., Cosnier, S., Silveira, C., Moura, J.J.G., Almeida, M.G., 2007. Electrochem. Commun. 9, 2241–2246.
Dave, B.C., Dunn, B., Valentine, J.S., Zink, J.I., 1994. Anal. Chem. 66, 1120A–1127A.
Dave, B.C., Miller, J.M., Dunn, B., Valentine, J.S., Zink, J.I., 1997. J. Sol-gel Sci. Technol. 8, 629–634.
Gorton, L., Lindgren, A., Larsson, T., Munteanu, F.D., Ruzgas, T., Gazaryan, I., 1999. Anal. Chim. Acta 400, 91–108.
Lev, O., Tsionsky, M., Rabinovich, L., Glezer, V., Sampath, S., Pankratov, I., Gun, J., 1995. Anal. Chem. 67, 22A–30A.
Moorcroft, M.J., Davis, J., Compton, R.G., 2001. Talanta 54, 785–803.
Pandey, P.C., Upadhyay, S., Pathak, H.C., 1999a. Electroanalysis 11, 59–64.
Pandey, P.C., Upadhyay, S., Pathak, H.C., Pandey, C.M.D., 1999b. Electroanalysis 11, 950–956.
Pandey, P.C., Upadhyay, S., Pathak, H.C., 1999c. Sens. Actuators B 60, 83–89.
Siebert, F., Hildebrandt, P., 2008. Vibrational Spectroscopy in Life Science. Wiley VCH Verlag GmbH & Co, Weinheim.
Silva, S., Cosnier, S., Almeida, M.G., Moura, J.G., 2004. Electrochem. Commun. 6, 404–408.
Wang, J., 1999a. J. Pharm. Biomed. Anal. 19, 47–53.
Wang, J., 1999b. Anal. Chim. Acta 399, 21–27.
Willner, B., Katz, E., Willner, I., 2006. Curr. Opin. Biotechnol. B 17, 589–596.
Wu, Y., Hu, S., 2007. Michrochim. Acta 159, 1–17.
Zhang, Z., Xia, S., Leonard, D., Jaffrezic-Renault, N., Zhang, J., Bessueille, F., Goepfert, Y.S., Wang, X., Chen, L., Zhu, Z., Zhao, J., Almeida, M.G., Silveira, C.M., 2009. Biosens. Bioelectron. 24, 1574–1579.